CHAPTER 9

Electrical Properties of Polymers, Ceramics, Dielectrics, and Amorphous Materials

9.1. Conducting Polymers and Organic Metals

Materials which are electrical (and thermal) insulators are of great technical importance and are, therefore, used in large quantities in the electronics industry, e.g., as handles for a variety of tools, as coatings for wires, or as casings for electrical equipment. Most polymeric materials have the required insulating properties and have been used for decades for this purpose. It came, therefore, as a surprise when it was discovered in the late 1970's that some polymers and organic substances may have electrical properties which resemble those of conventional semiconductors, metals, or even superconductors. We shall focus our attention mainly on these materials. This does not imply that the predominance of applications of polymers is in the conductor field. Quite the contrary is true. Nevertheless, conducting polymers (also called synthetic metals) steadily gain ground compared to insulating polymers.

Initially, conducting polymers were unstable in air or above room temperature. In addition, some dopants, used to impart a greater conductivity, were toxic, and the doping made the material brittle. However, more recently, stable conducting polymers were synthesized which have as an added benefit an optical transparency across the entire visible spectrum. Among them, poly(3,4-ethylenedioxythiophene) (**PEDOT**) and its derivatives enjoy now multi-ton productions, in particular for antistatic layers in photographic films. These conducting layers are beneficial for the prevention of friction-induced static electricity, which causes, on discharge, flashes of light, thus, pre-exposing the light-sensitive emulsion. Other uses of PEDOT are transparent electrodes for inorganic electroluminescent devices,

R.E. Hummel, *Electronic Properties of Materials 4th edition*,
DOI 10.1007/978-1-4419-8164-6_9,

anti-static treatments of plastics and cathode ray tubes, electrodes for capacitors, sensors, rechargeable batteries, photovoltaic devices, and packaging of electronic components. PEDOT films can be heated in air at 100°C for over 1000 hours with hardly any change in conductivity.

We now attempt to discuss conducting polymers in the light of solid-state physics. Conventional solid-state physics deals preferably with the properties of well-defined regular arrays of atoms. We have learned in Chapter 7 that a periodic array of lattice atoms is imperative for coherent scattering of electron waves and thus for a high conductivity. Further, the periodic arrangement of atoms in a crystal and the strong interactions between these atoms causes, as explained in Section 4.4, a widening of energy levels into energy bands.

We know that highly conducting materials such as metals are characterized by partially filled bands, which allow a free motion of the conduction electrons in an electric field. Insulators and semiconductors, on the other hand, possess (at least at 0 K) completely filled valence bands and empty conduction bands. The difference in band structure between crystalline insulators and semiconductors is a matter of degree rather than of kind: insulators have wide gaps between valence and conduction bands whereas the energy gaps for semiconductors are narrow. Thus, in the case of semiconductors, the thermal energy is large enough to excite some electrons across the gap into the conduction band. The conductivity in pure semiconductors is known to *increase* (exponentially) with increasing temperature and decreasing gap energy (8.14), whereas the conductivity in metals *decreases* with increasing temperature (Fig. 7.7). Interestingly enough, most conducting polymers have a temperature dependence of the conductivity similar to that of semiconductors. This suggests that certain aspects of semiconductor theory may be applied to conducting polymers. The situation regarding polymers cannot be described, however, without certain modifications to the band model brought forward in the previous chapters. This is due to the fact that polymeric materials may exist in amorphous as well as in crystalline form or, more commonly, as a mixture of both. This needs to be discussed in some detail.

Polymers consist of molecules which are long and chainlike. The atoms that partake in such a chain (or macromolecule) are regularly arranged along the chain. Several atoms combine and form a specific building block, called a monomer, and thousands of monomers combine to a polymer. As an example, we depict polyethylene, which consists of repeat units of one carbon atom and two hydrogen atoms, Fig. 9.1(a). If one out of four hydrogen atoms in polyethylene is replaced by a chlorine atom, polyvinylchloride (PVC) is formed upon polymerization (Fig. 9.1(b)). In polystyrene, one hydrogen atom is replaced by a benzene ring. More complicated macromolecules may contain side chains attached to the main link. They are appropriately named “branched polymers”. Macromolecules whose backbones consist largely of carbon atoms, as in Fig. 9.1, are called “organic” polymers.

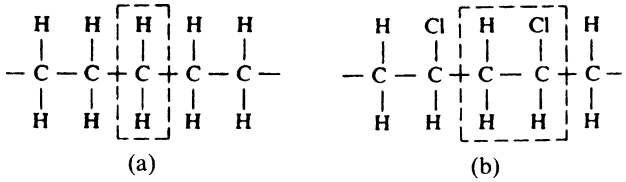

Figure 9.1. (a) Polyethylene. (b) Polyvinylchloride. (The dashed enclosures mark the repeat unit. Polyethylene is frequently depicted as two CH_2 repeat units for historical reasons).

The binding forces that hold the individual atoms in polymers together are usually covalent and sometimes ionic in nature. Covalent forces are much stronger than the binding forces in metals. They are based on the same interactions that are responsible for forming a hydrogen molecule from two hydrogen atoms. Quantum mechanics explains covalent bonds by showing that a lower energy state is achieved when two equal atomic systems are closely coupled and in this way exchange their energy (see Section 16.2). In organic polymers each carbon atom is often bound to four atoms (see Fig. 9.1) because carbon has four valencies.

In contrast to the strong binding forces between the atoms within a polymeric chain, the secondary interactions between the individual macromolecules are usually weak. The latter are of the Van der Waals type, i.e., they are based on forces which induce dipole moments in the molecules. (Similar weak interactions exist for noble gases such as argon, neon, etc.)

In order to better understand the electronic properties of polymers by means of the electron theory and the band structure concept, one needs to know the degree of order or the degree of periodicity of the atoms, because only ordered and strongly interacting atoms or molecules lead, as we know, to distinct and wide electron bands. Now, it has been observed that the degree of order in polymers depends on the length of the molecules and on the regularity of the molecular structure. Certain heat treatments may influence some structural parameters. For example, if a simple polymer is slowly cooled below its melting point, one might observe that some macromolecules align parallel to each other. The individual chains are separated by regions of supercooled liquid, i.e., of amorphous material (Fig. 9.2). Actually, slow cooling yields, for certain polymers, a highly crystalline structure.

In other polymers, the cooling procedure might cause the entire material to go into a supercooled-liquid state. In this state the molecules can be considered to be randomly arranged. After further cooling, below a glass transition temperature, the polymer might transform itself into a glassy amorphous solid which is strong, brittle, and insulating. However, as stated before, we shall concern ourselves mainly with polymers that have a high degree of crystallinity. Amorphous materials will be discussed in Section 9.4.

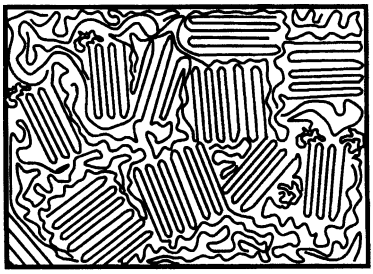

Figure 9.2. Simplified representation of a semicrystalline polymer (folded-chain model).

A high degree of crystallinity and a relatively high conductivity have been found in polyacetylene, which is the simplest **conjugated organic polymer**. It is considered to be the prototype of a conducting polymer. A conjugated polymer has alternating single and double bonds between the carbons (see Fig. 9.3, which should be compared to Fig. 9.1(a)). Two principal isomers are important: in the *trans* form, the hydrogen atoms are alternately bound to opposite sides of the carbons (Fig. 9.3(b)), whereas in the *cis* form the hydrogen atoms are situated on the same side of the double-bond carbons (Fig. 9.3(a)). **Trans-polyacetylene** is obtained as a silvery, flexible film that has a conductivity comparable to that of silicon (Fig. 9.4).

Figure 9.5 shows three band structures for *trans*-$(CH)_x$ assuming different distances between the carbon atoms. In Fig. 9.5(a) all carbon bond lengths are taken to be equal. The resulting band structure is found to be characteristic for a metal, i.e., one obtains distinct bands, the highest of which is *partially* filled by electrons. Where are the free electrons in the conduction band coming from? We realize that the electrons in the double bond of a conjugated polymer (called the π-electrons) can be considered to be only loosely bound to the neighboring carbon atoms. Thus, one of these electrons is easily disassociated from its carbon atom by a relatively small energy, which may be provided by thermal energy. The delocalized electrons may be accelerated as usual in an electric field.

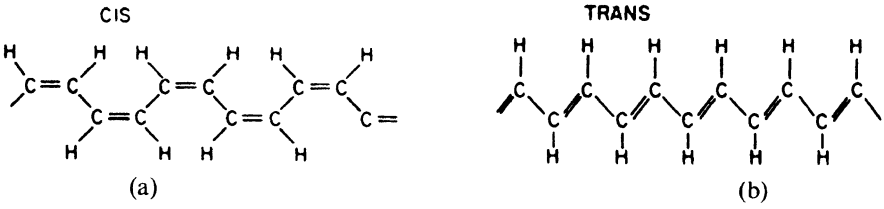

Figure 9.3. Theoretical isomers of polyacetylene (a) *cis*-transoidal isomer, (b) *trans*-transoidal isomer. Polyacetylene is synthesized as *cis*-$(CH)_x$ and is then isomerized into the *trans*-configuration by heating it at 150°C for a few minutes.

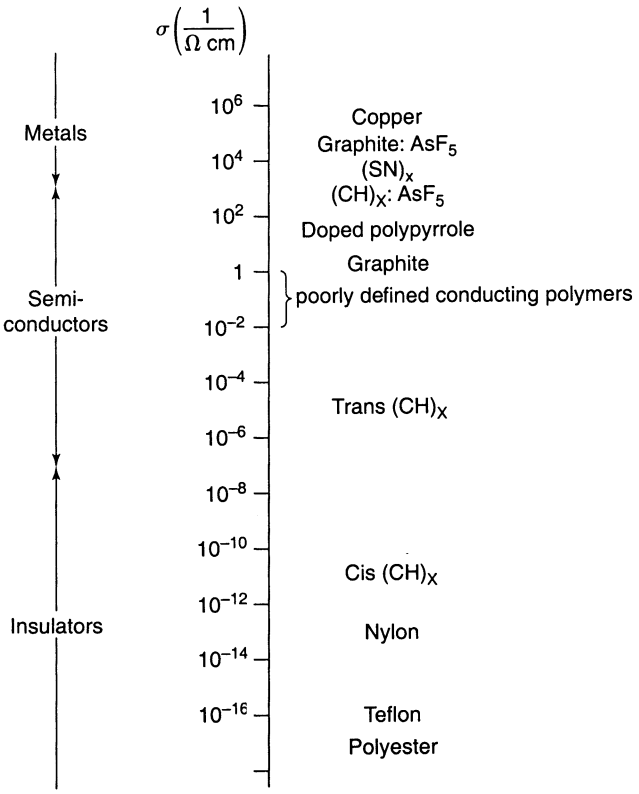

Figure 9.4. Conductivities of polymers in Ω^{-1} cm^{-1}. (Compare with Fig. 7.1.)

In reality, however, a uniform bond length between the carbon atoms does not exist in polyacetylene. Instead, the distances between the carbon atoms alternate because of the alternating single and double bonds. Band structure calculations for this case show, interestingly enough, some gaps between the individual energy bands. The resulting band structure is typical for a semiconductor (or an insulator)! The width of the band gap near the Fermi level depends mainly on the extent of alternating bond lengths (Fig. 9.5(b) and (c)).

It has been shown that the band structure in Fig. 9.5(b) best represents the experimental observations. Specifically, one finds a band gap of about 1.5 eV and a total width of the conduction band of 10–14 eV. The effective mass m^* is $0.6m_0$ at $k = 0$ and $0.1m_0$ at $k = \pi/a$. Assuming $\tau \rightarrow 10^{-14}$ s, the free carrier mobility, μ, along a chain is calculated to be about 200 cm^2/V s. The latter quantity is, however, hard to measure since the actual drift mobility in the entire solid is reduced by the trapping of the carriers which occurs during the "hopping" of the electrons between the individual macromolecules. In order to improve the conductivity of $(CH)_x$ one would attempt

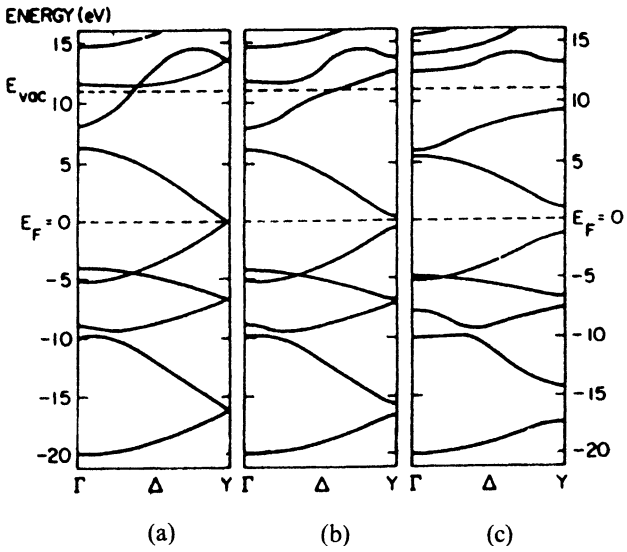

Figure 9.5. Calculated band structure of *trans*-$(CH)_x$ for different carbon–carbon bond lengths: (a) uniform (1.39 Å); (b) weakly alternating (C=C, 1.36 Å; C—C, 1.43 Å); and (c) strongly alternating (C=C, 1.34 Å; C—C, 1.54 Å). Note the band gaps at *Y* as bond alternation occurs. Reprinted with permission from P.M. Grant and I.P. Batra, *Solid State Comm*. **29**, 225 (1979).

to decrease the disparity in the carbon–carbon bond lengths, thus eventually approaching the uniform bond length as shown in Fig. 9.5(a).

*It should be noted in passing that chemists, particularly when dealing with organic molecules, utilize a different terminology for presenting the same information that has been just described. This will be briefly explained here for completeness. This alternative representation involves so-called **HOMO** and **LUMO** levels which are acronyms for *highest occupied molecular orbitals* and *lowest unoccupied molecular orbitals,* respectively. An **orbital** is described as a region in space about the nucleus in which there is a 95% probability of finding an electron, see Appendix 3. (Each of those orbitals can be occupied with maximal two electrons having opposite spin.) In short, the HOMO level is essentially analogous to (or better, a part of) the valence band, which we have used in previous chapters and in Fig. 9.5(b) and (c). Likewise, the LUMO level is part of the conduction band. The energy difference between the HOMO and LUMO levels is considered to be the band gap. Now, if there is an aggregate of molecules, the interaction between these individual molecules leads to a splitting of the HOMO and LUMO levels having slightly different energies. These sublevels have different vibrational energies. Once a large number of molecules are in close proximity, these energy levels overlap to form a continuum, that is, essentially an energy band.

A further piece of nomenclature may be added. In Appendix 3, we explain the meaning of σ and π orbitals. These binding orbitals are in their ground state and are therefore occupied by electrons. Once electrons are instead in an excited state they are termed to be in σ* and π* orbitals, respectively. Electron transitions between occupied orbitals and empty (excited) orbitals e.g. $\sigma \rightarrow \sigma^*$ or $n \rightarrow \pi^*$ (where n is a not-binding orbital above π and σ levels) can be achieved by providing the appropriate excitation energy (for example by impinging light). The π orbital is often set identical with the HOMO level and the π* orbital is equivalent to the LUMO level. As already mentioned above, the energy difference between the HOMO and LUMO levels, that is, the separation between π and π* orbitals is the band gap energy, $E_{g,}$ which is typically between 1 and 4 eV for organic semiconductors.

Polyacetylene, as discussed so far, should be compared to conventional intrinsic semiconductors. Now, we know from Section 8.3 that the conductivity of semiconductors can be substantially increased by doping. The same is true for polymer-based semiconductors. Indeed, arsenic–pentafluoride-doped trans-polyacetylene has a conductivity which is about seven orders of magnitude larger than undoped trans-$(CH)_x$. Thus, σ approaches the conductivity of metals, as can be seen in Figs. 9.4 and 9.6. Many oxidants cause

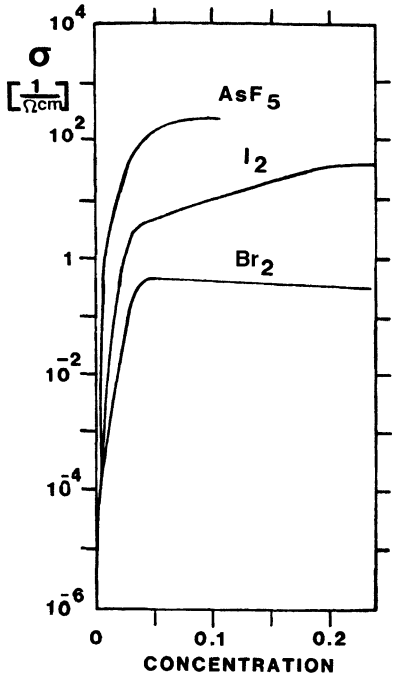

Figure 9.6. Conductivity change of polyacetylene as a result of doping.

p-type semiconductors, whereas alkali metals are *n*-type dopants. The doping is achieved through the vapor phase or by electrochemical methods. The dopant molecules diffuse between the $(CH)_x$ chains and provide a charge transfer between the polymer and the dopant. The additional element ends up as an anion when it is an acceptor and as a cation when it is a donor. Among other (albeit nontoxic) dopants is *n*-dodecyl sulfonate (soap). A word of caution, when using the word "doping", should be added at this point. In semiconductor physics, doping means extremely small additions of impurity elements. In polymers, much larger quantities of additional substances are used, ranging from one tenth of a percent up to 20–40%.

A refinement in the description of the conduction mechanism in polyacetylene can be provided by introducing the concept of **solitons**. A soliton is a structural distortion in a conjugated polymer and is generated when a single bond meets another single bond, as shown in Fig. 9.7. At the distortion point a localized nonbonding electron state is generated, similar to an *n*-type impurity state in a silicon semiconductor. In other words, a negative charge is associated with a soliton, as seen in Fig. 9.7 (involving two carbon bonds and one hydrogen bond to a carbon ion). The result is a localized level in the center of the forbidden band. It is believed that when an electron is excited from the valence band into the conduction band (leaving a hole in the valence band) this electron–hole pair decays in about 10^{-12} s into a more stable soliton–antisoliton pair.

Near the center of a soliton, the bond lengths are equal. We recall that uniform bond lengths constitute a metal. Thus, when many solitons have been formed and their spheres of influence overlap, a metal-like conductor would result.

It is also conceivable that one of the double bonds next to a soliton switches over to a single bond. If this switching occurs consecutively in one direction, a soliton wave results. This can be compared to a moving electron.

Up to now, we discussed mainly the properties of polyacetylene. Over the last 30 years additional conductive polymers have been discovered. They include polyanilines, polypyrroles, polythiophenes, polyphenylenes, poly(p-phenylene vinylene) and their derivatives. Of these, the **polyaniline** family can be easily processed at low cost but might yield toxic (carcinogenic) products upon degradation. Others are more "environmentally friendly" but are insoluble. On the other hand, the above-mentioned **PEDOT** (developed

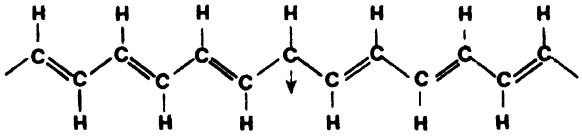

Figure 9.7. A broken symmetry in polyacetylene creates a *soliton*. (An *antisoliton* is the mirror image of a soliton.)

by Bayer AG in Germany) can be made water-soluble by utilizing poly (styrenesulfonate) (PSS) as a dopant during polymerization. Its antistatic and other properties have been mentioned already above. With respect to carbon-free polymers, the chains in inorganic **poly(sulfur nitride)** consist of alternating sulfur and nitrogen atoms. Because of the different valencies of the S^{2-} and N^{3-} ions, $(SN)_x$ is an electron-deficient material with an alternating bond structure. The bond length alternation is not severe, so that $(SN)_x$ has a room-temperature **conductivity of about 10^3 ohm^{-1} cm^{-1} along the chain direction. The conductivity increases with** a reduction in temperature. At temperatures close to 0 K, poly(sulfur nitride) becomes superconducting. In brominated $(SN)_x$ the Br_3^- and Br_2^- ions are aligned along the chain axis, giving rise to a one-dimensional superlattice.

In **graphite**, "molecules" consists of "sheets" of carbon atoms. The conductivity is found to be nearly metallic, at least parallel to the layers (Fig. 9.4). AsF_5-doped graphite has an even higher conductivity. The conduction is increased by producing a mixture of easily ionized electron donors and electron acceptors. The charge is then shared between the donors and acceptors. These materials are called charge-transfer complexes.

An isolated atomic plane of graphite, that is, a monolayer of carbon atoms, is called **graphene**. It can be identified in the high-resolution electron microscope as a two-dimensional (2D) honeycomb lattice (six-member carbon ring), where the distance between next-neighbor atoms is 0.14 nm. Graphene has extraordinary physical properties and is therefore intensely studied both, from a theoretical point of view as well as experimentally because of its potential applications in computer technology and other fields. Specifically, intrinsic graphene is a semi-metal whereas extrinsic graphene is a semiconductor whose band gap can be tuned from 0 to 0.25 eV. It has a zero effective mass for electrons and holes at low energies, a high room temperature electron mobility (>1.5 m^2/V s, compared to 0.15 m^2/V s for Si, see Appendix 4) leading to a mean free path of several microns, a sheet conductivity of 10^6 1/(Ω cm) (which is larger than that for Ag, see Fig. 7.1), and a thermal conductivity around 5×10^3 W/m K (which is higher than that for diamond, see Table 19.3). Moreover, graphene seems to be one of the strongest materials, having a breaking strength 200 times larger than steel. It absorbs about 2.3% of white light despite its monolayer thickness (which makes it visible in transmission). Finally, the quantum Hall effect has been observed in graphene at room temperature (see Section 8.5). No wonder that it is speculated that graphene would eventually replace silicon for ultra-large-scale integrated electronic devices. Indeed, n-and p-type semiconductors, a bipolar transistor, a field-effect transistor, operating at 100 GHz, hundreds of transistors on a single flake, and a frequency multiplier, have been already demonstrated. Among further potential applications are ultra capacitors, sensors, and transparent, conducting electrodes for organic light emitting diodes, organic photovoltaic cells (Section 13.8.15), touch-screens, and liquid crystal displays (Section 13.8.16).

If this sounds like a miracle material, one has to admit that the fabrication of graphene is not a trivial task. Several techniques have been successfully (and unsuccessfully) tried, which have so far yielded only small quantities of pristine graphene (flakes about 1 mm^2 in size) or larger sheets of lesser quality. Among them is the initial Scotch tape technique involving repeated splitting of graphite crystals into increasingly thinner segments, which, after dissolving the tape in acetone, are sedimented on a Si wafer. An alternative is the dry deposition method, also called the drawing technique (because drawing a line with a graphite pencil also yields flakes of graphene). A further method involves heating silicon carbide at about 1,400°C to reduce it to graphene.

Historically, extremely thin graphitic flakes have been described in 1962 and a few layers of graphene were observed in the TEM in 1948. The term *graphene* first appeared in 1987 to describe graphite intercalation compounds. Eventually, the "mechanical exfoliation" of graphite to stable, electronically isolated graphene, in 2004 by Geim and Novoselov, as described above, led to the rush of experimental and theoretical endeavors involving scientific labs all over the world. Progress in this field should be followed with great anticipation.

Another class of conductors is the **charge-transfer salts**, in which a donor molecule, such as tetrathiafulvalene (TTF), transfers electrons to an acceptor molecule, such as tetracyanoquinodimethane (TCNQ). The planar molecules stack on top of each other in sheets, thus allowing an overlap of wave functions and a formation of conduction bands that are partially filled with electrons due to the charge transfer. It is assumed that, because of the sheetlike structure, the charge-transfer compounds are quasi-one-dimensional. Along the stacks, conductivities as high as $2 \times 10^3\ \Omega^{-1}\ cm^{-1}$ have been observed at room temperature. Below room temperature, the metallic conductors often transform into semiconductors or insulators. Even superconduction has been observed at very low temperatures (about 13 K). In the presence of a magnetic field and at low temperatures, these materials undergo, occasionally, a transition from a metallic, nonmagnetic state into a semimetallic, magnetic state. Organic metals are generally prepared by electrochemical growth in a solution. They are, as a rule, quite brittle, single crystalline, and relatively small. Other materials of this type include doped complexes of C_{60} (so-called Buckyballs) which exhibit superconductivity at low temperatures.

Replacing metals with lightweight conducting polymers (for wires) seems to be, in the present state of the art, nearly impossible, mainly because of their poor stability. However, this very drawback (i.e., the high reactivity of some conducting polymers) concomitant with a change in conductivity can be profitably utilized in devices such as remote gas sensors, biosensors, or other remotely readable indicators that detect changes in humidity, radiation dosage, mechanical abuse, or chemical release. As an example,

polypyrrole noticeably changes its conductivity when exposed to only 0.1% NH_3, NO_2, or H_2S. Further, experiments have been undertaken to utilize $(CH)_x$ for measuring the concentration of glucose in solutions.

9.2. Ionic Conduction

In ionic crystals (such as the alkali halides), the individual lattice atoms transfer electrons between each other to form positively charged cations and negatively charged anions. The binding forces between the ions are electrostatic in nature and are thus very strong. The room-temperature conductivity of ionic crystals is about twenty-two orders of magnitude smaller than the conductivity of typical metallic conductors (Fig. 7.1). This large difference in σ can be understood by realizing that the wide band gap in insulators allows only extremely few electrons to become excited from the valence band into the conduction band.

The main contribution to the electrical conduction in ionic crystals (as little as it may be) is, however, due to a mechanism that we have not yet discussed, namely, ionic conduction. Ionic conduction is caused by the movement of some negatively (or positively) charged ions which *hop* from lattice site to lattice site under the influence of an electric field, see Fig. 9.8 (b). (This type of conduction is similar to that which is known to occur in aqueous electrolytes.) This ionic conductivity

$$\sigma_{\text{ion}} = N_{\text{ion}} e \mu_{\text{ion}} \tag{9.1}$$

is, as outlined before (8.13), the product of three quantities. In the present case, N_{ion} is the number of ions per unit volume that can change their position under the influence of an electric field and μ_{ion} is the mobility of these ions.

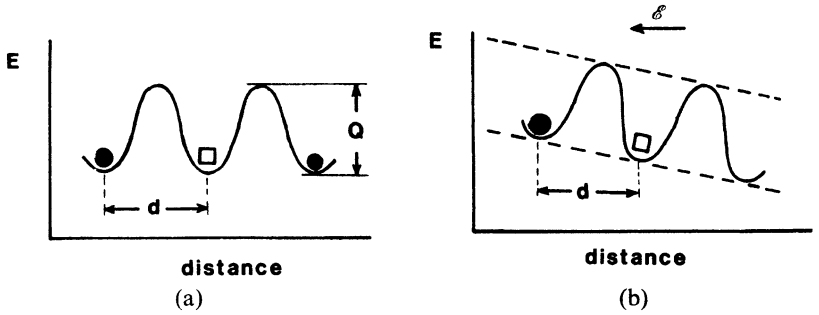

Figure 9.8. Schematic representation of a potential barrier, which an ion (●) has to overcome to exchange its site with a vacancy (□). (a) Without an external electric field; (b) with an external electric field. d = distance between two adjacent, equivalent lattice sites; Q = activation energy.

In order for ions to move through a crystalline solid, they must have sufficient energy to pass over an *energy barrier* (Fig. 9.8). Further, an equivalent lattice site next to a given ion must be empty in order for an ion to be able to change its position. Thus, N_{ion} in (9.1) depends on the vacancy concentration in the crystal (i.e., on the number of *Schottky defects*[17]). In short, the theory of ionic conduction contains essential elements of diffusion theory, with which the reader might be familiar.

Diffusion theory links the mobility of the ions, which is contained in (9.1), with the diffusion coefficient, D, through the Einstein relation,

$$\mu_{\text{ion}} = \frac{De}{k_{\text{B}}T}. \tag{9.2}$$

(Note that (9.2) implies that *one* charge unit per atom is transported.)

The diffusion coefficient varies with temperature; this dependence is commonly expressed by an Arrhenius equation,

$$D = D_0 \exp\left[-\left(\frac{Q}{k_{\text{B}}T}\right)\right], \tag{9.3}$$

where Q is the activation energy for the process under consideration (Fig. 9.8), and D_0 is a pre-exponential factor that depends on the vibrational frequency of the atoms and some structural parameters. Combining (9.1) through (9.3) yields

$$\sigma_{\text{ion}} = \frac{N_{\text{ion}}e^2 D_0}{k_{\text{B}}T} \exp\left[-\left(\frac{Q}{k_{\text{B}}T}\right)\right]. \tag{9.4}$$

Equation (9.4) is shortened by combining the pre-exponential constants into σ_0:

$$\sigma_{\text{ion}} = \sigma_0 \exp\left[-\left(\frac{Q}{k_{\text{B}}T}\right)\right]. \tag{9.5}$$

Taking the natural logarithm yields

$$\ln \sigma_{\text{ion}} = \ln \sigma_0 - \left(\frac{Q}{k_{\text{B}}}\right)\frac{1}{T}. \tag{9.6}$$

Equation (9.6) suggests that if $\ln \sigma_{\text{ion}}$ is plotted versus $1/T$, a straight line with a negative slope would result. Figure 9.9 depicts schematically a plot of $\ln \sigma$ versus $1/T$ as experimentally found for alkali halides. The linear $\ln \sigma$ versus $1/T$ relationship indicates that Fig. 9.9 is an actual representation

[17] A *Schottky defect* is formed when an anion as well as a cation of the same absolute valency are missing (to preserve charge neutrality).

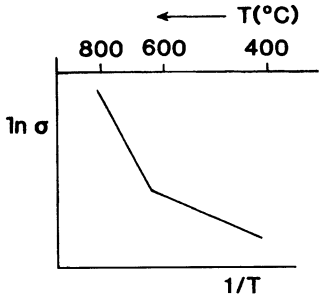

Figure 9.9. Schematic representation of ln σ versus $1/T$ for Na^+ ions in sodium chloride. (Arrhenius plot).

of (9.6). The slopes of the straight lines in Arrhenius plots are utilized to calculate the activation energy of the processes under consideration. We notice in Fig. 9.9 two temperature regions representing two different activation energies: at low temperatures, the activation energy is small, the thermal energy is just sufficient to allow the hopping of ions into already existing vacancy sites. This temperature range is commonly called the **extrinsic region**. On the other hand, at high temperatures, the thermal energy is large enough to create additional vacancies. The related activation energy is thus the sum of the activation energies for vacancy creation and ion movement. This temperature range is called the **intrinsic region**.

So far, we have not been very specific in describing the circumstances of vacancy formation in an ionic crystal. Now, we have to realize that whenever vacant lattice sites are created, an overall charge neutrality needs to be maintained. The latter is the case when both a cation and an anion are removed from a lattice. Another permissible mechanism is the formation of a vacancy-interstitial pair (**Frenkel defect**). More often, however, vacancies are created as a consequence of introducing differently charged impurity atoms into an ionic lattice, i.e., by replacing, say, a monovalent metal atom with a divalent atom. In order to maintain charge neutrality in this case, a positively charged vacancy needs to be introduced. For example, if a divalent Mg^{2+} ion substitutes for a monovalent Na^+ ion, one extra Na^+ ion has to be removed to restore charge neutrality, see Fig. 9.10. Or, if zirconia (ZrO_2) is treated with CaO (to produce the technically important **calcia-stabilized zirconia**), the Ca^{2+} ions substitute for Zr^{4+} ions and an anion vacancy needs to be created to maintain charge neutrality. Nonstoichiometric compounds contain a high amount of vacancies even at relatively low temperatures, whereas in stoichiometric compounds vacancies need to be formed by elevating the temperature.

In principle, both cations and anions are capable of moving simultaneously under the influence of an electric field. It turns out, however, that in most alkali halides the majority carriers are provided by the (smaller)

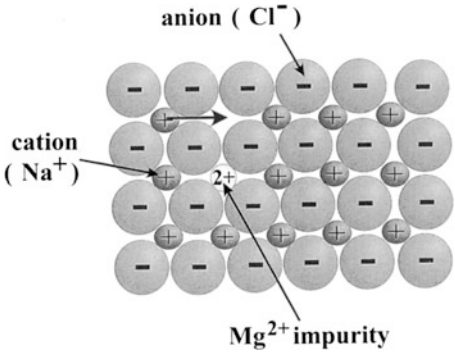

Figure 9.10. Schematic representation of a {100} plane of an ionic crystal having the NaCl structure. The diffusion of a cation into a cation vacancy is shown. Also depicted is the creation of a cation vacancy when replacing a Na^+ ion with a Mg^{2+} ion.

metal ions, whereas in other materials, such as the lead halides, the conduction is predominantly performed by the halide ions.

So far, it was implied that the materials under consideration are single crystals. For polycrystalline materials, however, it appears reasonable to assume that the vacant lattice sites provided by the grain boundaries would be utilized by the ions as preferred paths for migration, thus enhancing the conductivity. This has indeed been experimentally observed for alkali ions.

One piercing question remains to be answered: If ionic conduction entails the transport of ions, i.e., of matter from one electrode to the other, would this not imply some segregation of the constituents? Indeed, a pile-up of mobile ions at the electrodes has been observed for long-lasting experiments with a concomitant induced electric field in the opposite direction to the externally applied field. As a consequence the conductivity decreases gradually over time. Of course, this does not happen when nonblocking electrodes are utilized which provide a source and a sink for the mobile species.

9.3. Conduction in Metal Oxides

Metal oxides do not actually represent a separate class of conducting materials on their own. Indeed, they can be insulating, such as $\mathbf{TiO_2}$, have metallic conduction properties, such as **TiO**, or be semiconducting. For understanding the mechanisms involved in metal oxides, e.g., in the aforementioned titanium oxides, it is helpful to inspect the table in Appendix 3. Oxygen is seen there to have four 2*p*-electrons in its outermost shell. Two more electrons will bring O^{2-} into the closed-shell configuration and four electrons are obviously needed to accomplish the same for two oxygen ions,

such as in TiO_2. These four electrons are provided by the titanium from its 3*d*- and 4*s*-shells. Thus, in the case of TiO_2, all involved elements are in the noble gas configuration. Since ionic bonds are involved, any attempted removal of electrons would require a considerable amount of thermal energy. TiO_2 is, consequently, an insulator having a wide band gap. Not so for TiO. Since only two titanium valence electrons are needed to fill the 2*p*-shell of *one* oxygen ion, two more titanium electrons are free to serve as conduction electrons. Thus, TiO has metallic properties with a σ in the $10^3\ \Omega^{-1}\ cm^{-1}$ range.

A refinement of our understanding is obtained by considering the pertinent electron bands. TiO has, according to the aforementioned explanations, a filled oxygen 2*p*-valence band and an essentially empty titanium 4*s*-conduction band. Also involved is a narrow titanium 3*d*-band which is partially filled by the above-mentioned two electrons. The conduction in TiO takes place, therefore, in the titanium 3*d*-band, which can host, as we know, a total of 10 electrons.

We discuss **zinc oxide** as a next example. Zn in ZnO has two valence 4*s*-electrons which transfer to the oxygen 2*p*-band. ZnO, if strictly stoichiometric, has, thus, a filled valence 2*p*-band and an empty zinc 4*s*-band employing a gap energy of 3.3 eV. Stoichiometric ZnO is therefore an insulator or a wide-band-gap semiconductor. Now, if interstitial zinc atoms (or oxygen vacancies) are introduced into the lattice (by heating ZnO in a reducing atmosphere, which causes neutral oxygen to leave the crystal) then the valence electrons of these zinc interstitials are only loosely bound to their nuclei. One of these two electrons can easily be ionized (0.05 eV) and acts therefore as a donor. Nonstoichiometric ZnO is, consequently, an *n*-type semiconductor. The same is incidentally true for nonstoichiometric Cu_2O (see Appendix 3), an established semiconducting material from which Cu/Cu_2O Schottky-type rectifiers were manufactured long before silicon technology was invented.

Another interesting metal oxide is SnO_2 (sometimes doped with In_2O_3), which is transparent in the visible region and which is a reasonable conductor in the $1\ \Omega^{-1}\ cm^{-1}$ range. It is used in optoelectronics to provide electrical contacts without blocking the light from reaching a device. It is known as **indium-tin-oxide or ITO**.

Finally, we discuss **NiO**. Again, a filled oxygen 2*p*-band and an empty nickel 4*s*-band are involved. In order to form the nickel 3*d*-bands required for conduction, a substantial overlap of the 3*d*-wave functions would be required by quantum mechanics. Band structure calculations show, however, that these interactions do not take place. Instead, *deep-lying localized electron states* in the forbidden band close to the upper edge of the valence band are observed. Thus, no 3*d*-band conduction can take place, which results in stoichiometric NiO being an insulator. Nonstoichiometry (obtained by removing some nickel atoms, thus creating cation vacancies) causes NiO to become a *p*-type semiconductor.

9.4. Amorphous Materials (Metallic Glasses)

Before we discuss electrical conduction in amorphous materials, we need to clarify what the term *amorphous* means in the present context. Strictly speaking, *amorphous* implies the random arrangement of atoms, the absence of any periodic symmetry, or the absence of any crystalline structure. One could compare the random distribution of atoms with the situation in a gas, as seen in an instantaneous picture. Now, such a completely random arrangement of atoms is seldom found even in liquids, much less in solids. In actuality, the relative positions of nearest neighbors surrounding a given atom in an amorphous solid are almost identical to the positions in crystalline solids because of the ever-present binding forces between the atoms. In short, the atomic order in amorphous materials is restricted to the nearest neighbors. Amorphous materials exhibit, therefore, only *short-range order*. In contrast to this, the exact positions of the atoms that are farther apart from a given central atom cannot be predicted. This is particularly the case when various kinds of stacking orders, i.e., if polymorphic modifications, are possible. As a consequence one observes atomic disorder at long range. The term *amorphous solid* should therefore be used *cum grano salis*. We empirically define materials to be amorphous when their diffraction patterns consist of diffuse rings, rather than sharply defined Bragg rings, as are characteristic for polycrystalline solids.

So far we have discussed **positional disorder** only as it might be found in pure materials. If more than one component is present in a material, a second type of disorder is possible: The individual species might be randomly distributed over the lattice sites; i.e., the species may not be alternately positioned as is the case for, say, sodium and chlorine atoms in NaCl. This random distribution of species is called **compositional disorder**.

The best-known representative of an amorphous solid is window glass, whose major components are silicon and oxygen. Glass is usually described as a supercooled liquid.

Interestingly enough, many elements and compounds that are generally known to be crystalline under equilibrium conditions can also be obtained in the nonequilibrium amorphous state by applying rapid solidification techniques, i.e., by utilizing cooling rates of about 10^5 K/s. These cooling rates can be achieved by fast quenching, melt spinning, vapor deposition, sputtering, radiation damage, filamentary casting in continuous operation, spark-processing, etc. The degree of amorphousness (or, the degree of short range order) may be varied by the severity of the quench. The resulting **metallic glasses**, or *glassy metals*, have unusual electrical, mechanical, optical, magnetic, and corrosion properties and are therefore of considerable interest. Amorphous semiconductors (consisting, e.g., of Ge, Si, GeTe, etc.) have also received substantial attention because they are relatively inexpensive to

manufacture, have unusual switching properties, and have found applications in inexpensive photovoltaic cells.

We now turn to the atomic structure of amorphous metals and alloys. They have essentially nondirectional bonds. Thus, the short-range order does not extend beyond the nearest neighbors. The atoms must be packed together tightly, however, in order to achieve the observed density. There are only a limited number of ways of close packing. One way of arranging the atoms in amorphous metals is depicted by the *dense random packing of hard spheres* model (Fig. 9.11). This **Bernal model** is considered as the ideal amorphous state. No significant regions of crystalline order are present. In transition metal–metalloid compounds (such as Ni–P) it is thought that the small metalloid atoms occupy the holes which occur as a consequence of this packing (**Bernal–Polk model**).

The atoms in amorphous semiconductors, on the other hand, do not arrange themselves in a close-packed manner. Atoms of group IV elements are, as we know, covalently bound. They are often arranged in a *continuous random network* with correlations in ordering up to the third or fourth nearest neighbors (Fig. 9.12(b) and (c)). Amorphous pure silicon contains numerous *dangling bonds* similar to those found in crystalline silicon in the presence of vacancies (Fig. 9.12(a)).

Since amorphous solids have no long-range crystal symmetry, we can no longer apply the Bloch theorem, which led us in Section 4.4 from the distinct energy levels for isolated atoms to the broad quasi-continuous bands for crystalline solids. Thus, the calculation of electronic structures for amorphous metals and alloys has to use alternate techniques, e.g., the **cluster model** approach. This method has been utilized to calculate the electronic structure of amorphous Zr–Cu (which is a representative of a noble metal–transition metal metallic glass). A series of clusters were assumed which

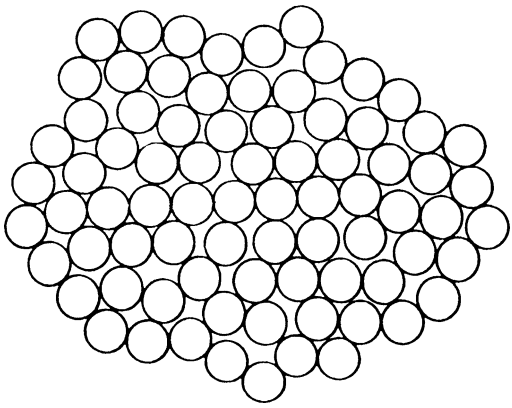

Figure 9.11. Two-dimensional schematic representation of a dense random packing of hard spheres (Bernal model).

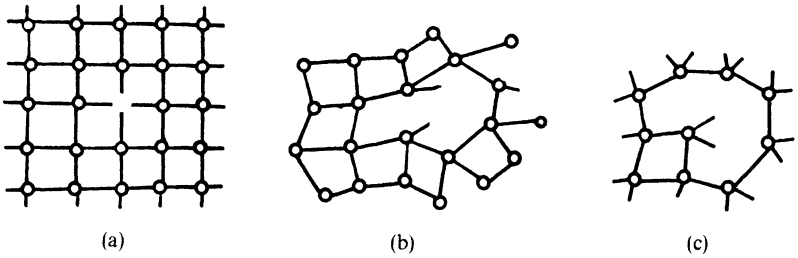

Figure 9.12. Defects in crystalline and amorphous silicon. (a) Monovacancy in a crystalline semiconductor; (b) one and (c) two dangling bonds in a continuous random network of an amorphous semiconductor. (Note the deviations in the interatomic distances and bond angles).

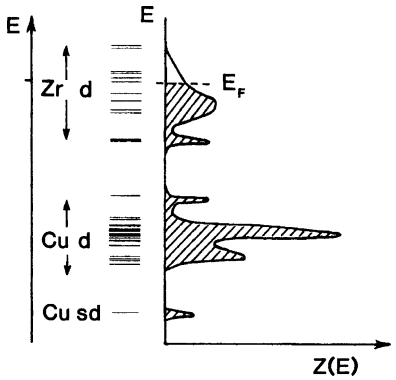

Figure 9.13. Schematic representation of the molecular orbital energy level diagram and the density of states curves for Zr–Cu clusters. The calculated density of states curves agree reasonably well with photoemission experiments.

exhibit the symmetry of the close-packed lattices fcc (as for Cu) and hcp[18] (as for Zr). The energy level diagram depicted in Fig. 9.13 shows two distinct "bands" of levels. The lower band consists primarily of copper *d*-levels, while the upper band consists mainly of zirconium *d*-levels. A sort of gap separates the two bands of levels. Even though the concept of quasi-continuous energy bands is no longer meaningful for amorphous solids, the density of states concept still is, as can be seen in Fig. 9.13. We notice that the Fermi energy is located in the upper part of the zirconium levels. Further, we observe partially filled electron states. This has two interesting consequences. First, we expect *metal-like* conduction. Second, $Z(E)$ near E_F is small, which suggests relatively small values for the

[18] Hexagonal close-packed.

conductivity (see (7.26)). Indeed, σ for Cu–Zr is comparable to that of poor metallic conductors (i.e., approximately 5×10^3 1/Ω cm).

The electrical resistivity of many metallic glasses (such as $Pd_{80}Si_{20}$ or $Fe_{32}Ni_{36}Cr_{14}P_{12}B_6$[19]) stays constant over a fairly wide temperature range, up to the temperature which marks the irreversible transition from the amorphous into the crystalline state. This makes these alloys attractive as resistance standards. The mean free path for electrons in metallic glasses is estimated to be about 1 nm.

The energy level diagrams and the density of states curves for **amorphous semiconductors** are somewhat different from those for amorphous metals. Because of the stronger binding forces which exist between the atoms in covalently bound materials, the valence electrons are tightly bound, or *localized*. As a consequence, the density of states for the localized states extends into the "band gap" (Fig. 9.14). This may be compared to the localized impurity states in doped crystalline semiconductors, which are also located in the band gap. Thus, we observe density of states *tails*. These tails may extend, for some materials, so far into the gap that they partially overlap. In general, however, the density of electron and hole states for the localized levels is very small.

The electrical conductivity for amorphous semiconductors, σ_A, depends, as usual (8.13), on the density of carriers, N_A, and the mobility of these carriers, μ_A:

$$\sigma_A = N_A e \mu_A. \tag{9.7}$$

The density of carriers in amorphous semiconductors is extremely small, because all electrons are, as said before, strongly bound (localized) to their

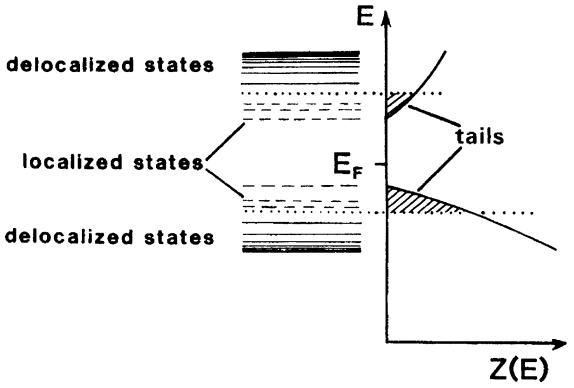

Figure 9.14. Localized and delocalized states and density of states $Z(E)$ for amorphous semiconductors. Note the band tails, which are caused by the localized states.

[19] METGLAS 2826A, trademark of Allied Chemical.

respective nuclei. Likewise, the mobility of the carriers is small because the absence of a periodic lattice causes substantial incoherent scattering. As a consequence, the room-temperature conductivity in amorphous semiconductors is generally very low (about 10^{-7} 1/Ω cm).

Some of the localized electrons might occasionally acquire sufficient thermal energy to overcome barriers which are caused by potential wells of variable depth and hop to a neighboring site. Thus, the conduction process in amorphous semiconductors involves a (temperature-dependent) activation energy, Q_A, which leads to an equation similar to (9.5), describing a so-called variable-range hopping

$$\sigma_A = \sigma_0 \exp\left[-\left(\frac{Q_A(T)}{k_B T}\right)\right]. \tag{9.8}$$

Equation (9.8) states that the conductivity in amorphous semiconductors increases exponentially with increasing temperature, because any increase in thermal energy provides additional free carriers.

The application of amorphous silicon for *photovoltaic devices* (see Section 8.7.6) will be discussed briefly in closing because of its commercial, as well as scientific, significance. If silicon is deposited out of the gas phase on relatively cold (<500°C) substrates (utilizing silane or sputtering), a structure as shown in Fig. 9.12 (b) and (c) results. Doping is virtually not possible in this condition since any free charge carriers recombine immediately with the dangling bonds. However, hydrogen, if added during deposition and incorporated into the solid, neutralizes the unsaturated valencies (and reduces internal strain in the lattice network). This results in **hydrogenated amorphous silicon**, which is, in its properties, quite comparable to crystalline silicon. Doping can be accomplished during deposition. This way, semiconducting materials can be produced which vary in their conductivity between 10^{-11} and 10^{-2} Ω^{-1} cm^{-1} depending on doping (see Fig. 7.1). Commercial flat-plate solar cells of this type have an efficiency of about 8% compared to 14% efficiency for commercial single-crystal silicon technology. The price (and the consumption of power during manufacturing) is, however, only one-half of that for crystalline silicon, mainly because of the simpler way of deposition (see Section 8.7.6).

The understanding of amorphous metals, alloys, and semiconductors is still in its infancy. Future developments in this field should be followed with a great deal of anticipation because of the potentially significant applications which might arise in the years to come.

9.4.1. Xerography

Xerography (from the Greek "dry writing") or **electrophotography** is an important application of amorphous semiconductors such as amorphous

selenium or amorphous silicon, etc. (They have been recently replaced, however, by *polyvinylcarbazole*.) Such a material, when deposited on a cylindrically shaped metallic substrate, constitutes the *photoreceptor* drum, as shown in Fig. 9.15.

Before copying, the photoreceptor is electrostatically charged by means of a corona wire to which a high voltage is applied (Step 1). Amorphous semiconductors are essentially insulators (see above) which hold this electric charge reasonably well, as long as they are kept in the dark. If, however, light which has been reflected from the document to be copied falls on the photoreceptor, electron–hole pairs are formed, causing the photoreceptor to become conducting. This process discharges the affected parts on the drum, creating a latent image on the photoreceptor, i.e., a pattern consisting of charged and neutral areas. At the next step, electrostatically charged and pigmented polymer particles (called *toner*) are brought into contact with the drum. The toner clings to the charged areas only. Commonly, a two-component toner is utilized; one part consists of magnetically soft particles. They form brush-type chains under the influence of a magnetic field which is caused by permanent magnets that are rotated inside a cylinder (see Fig. 9.15, Step 3). Eventually, the toner on the photoreceptor is electrostatically transferred to a piece of paper by properly corona-charging the back

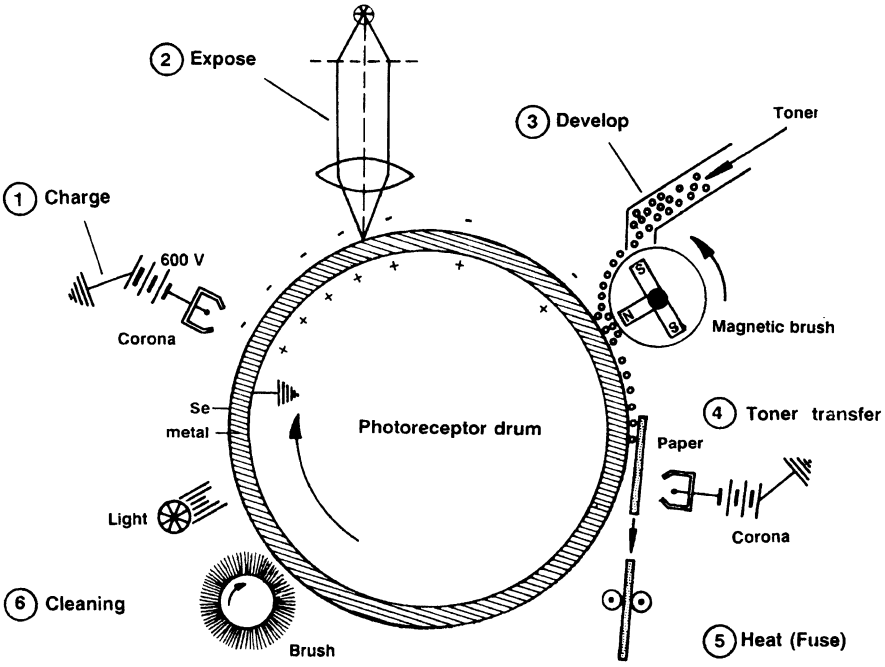

Figure 9.15. Schematic representation of the electrophotography process. The individual steps are explained in the text.

of the paper. Finally, the toner is fused to the paper by heat. A cleaning and photodischarging process prepares the photoreceptor drum for the next cycle.

Laser printers use the same principle. To create the latent image, the laser light is periodically scanned across the rotating photoreceptive drum by means of a rotating multisurface mirror. The spectral sensitivity of the amorphous semiconductor has to be matched to the wavelength of the laser light. Amorphous silicon (maximal photosensitivity near 700 nm) in conjunction with a helium–neon laser (see Table 13.1) is a usable combination.

9.5. Dielectric Properties

Insulators (also often called dielectric materials) possess a number of additional important electrical properties that make them useful in the electronics industry. They will be explained in this section.

When a voltage is momentarily applied to two parallel metal plates which are separated by a distance, L, as shown in Fig. 9.16, then the resulting electric charge essentially remains on these plates even after the voltage has been removed (at least as long as the air is dry). This ability to store an electric charge is called **capacitance**, C, which is defined to be the charge, q, per unit applied voltage, V, that is:

$$C = \frac{q}{V}, \tag{9.9}$$

where C is given in coulombs per volt, or farad (see Appendix 4). Understandably, the capacitance is higher the larger the area, A, of the plates and the smaller the distance, L, between them. Further, the capacitance depends

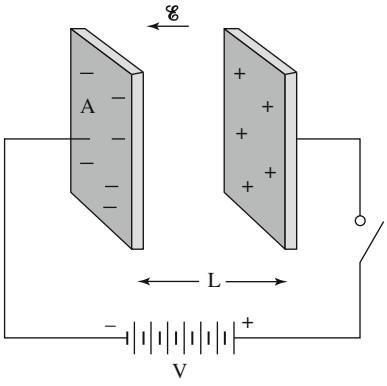

Figure 9.16. Two metal plates, separated by a distance, L, can store electric energy after having been charged momentarily by a battery.

on the material that may have been inserted between the plates. The experimental observations lead to

$$C = \varepsilon\varepsilon_0 \frac{A}{L}, \tag{9.10}$$

where

$$\varepsilon = \frac{C}{C_{\text{vac}}} \tag{9.11}$$

determines the magnitude of the added storage capability. It is called the (unitless) **dielectric constant** (or occasionally the *relative permittivity*, ε_r). ε_0 is a universal constant having the value of 8.85×10^{-12} farad per meter (F/m), or As/Vm, and is known by the name **permittivity of empty space** (or of vacuum). Some values for the dielectric constant are given in Table 9.1. The dielectric constant of empty space is set to be 1, whereas ε of air and many other gases is nearly 1. The dielectric constant is frequency dependent.

We now need to explain why the capacitance increases when a piece of a dielectric material is inserted between two conductors [see Eq. (9.10)]. For this, one has to realize that, under the influence of an external electric field, the negatively charged electron cloud of an atom becomes displaced with

Table 9.1. DC Dielectric Constants of Some Materials

Potassium tantalate niobate	6,000	
Barium titanate ($BaTiO_3$)	4,000	Ferroelectric
Potassium Niobate ($KNbO_3$)	700	
Rochelle salt ($NaKC_4H_4O_6 \cdot 4H_2O$)	170	
Water	81.1	
Acetone	20	
Silicon	11.8	
GaAs	10.9	
Marble	8.5	
Soda-lime-glass	6.9	
Porcelain	6.0	
Epoxy	4.0	
Fused silica	4.0	Dielectric
Nylon 6,6	4.0	
PVC	3.5	
Ice	3.0	
Amber	2.8	
Polyethylene	2.3	
Paraffin	2.0	
Air	1.000576	

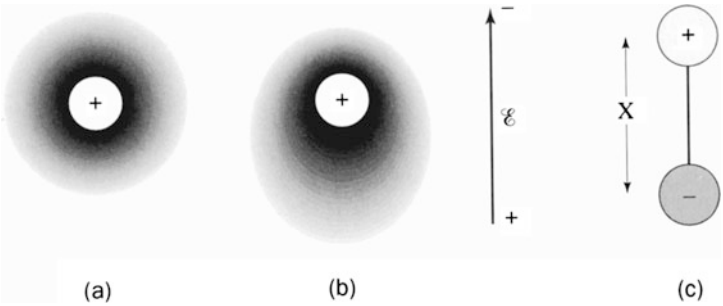

Figure 9.17. An atom is represented by a positively charged core and a surrounding, negatively charged, electron cloud (a) in equilibrium and (b) in an external electric field. (c) Schematic representation of an electric dipole as, for example, created by separation of the negative and positive charges by an electric field, as seen in (b).

respect to its positively charged core; compare Fig. 9.17(a) with (b). As a result, a dipole is created, which has an **electric dipole moment**

$$p = q \cdot x, \tag{9.12}$$

where x is the separation between the positive and the negative charge as depicted in Fig. 9.17(c). (The dipole moment is generally a vector pointing from the negative to the positive charge.) The process of dipole formation (or alignment of already existing dipoles) under the influence of an external electric field that has an electric field strength, $\mathscr{E}$, is called **polarization**. Dipole formation of all involved atoms within a dielectric material causes a charge redistribution so that the surface nearest to the positive capacitor plate is negatively charged (and vice versa), see Fig. 9.18(a). As a consequence, electric field lines within a dielectric are created which are opposite in direction to the external field lines. Effectively, the electric field lines within a dielectric material are weakened due to polarization, as depicted in Fig. 9.18(b). In other words, the **electric field strength** in a material,

$$\mathscr{E} = \frac{\mathscr{E}_{\text{vac}}}{\varepsilon}, \tag{9.13}$$

is reduced by inserting a dielectric between two capacitor plates.

Within a dielectric material the electric field strength, $\mathscr{E}$, is replaced by the **dielectric displacement**, D (also called the *surface charge density*), that is,

$$D = \varepsilon\varepsilon_0\mathscr{E} = \frac{q}{A}. \tag{9.14}$$

The dielectric displacement is the superposition of two terms:

$$D = \varepsilon_0\mathscr{E} + P, \tag{9.15}$$

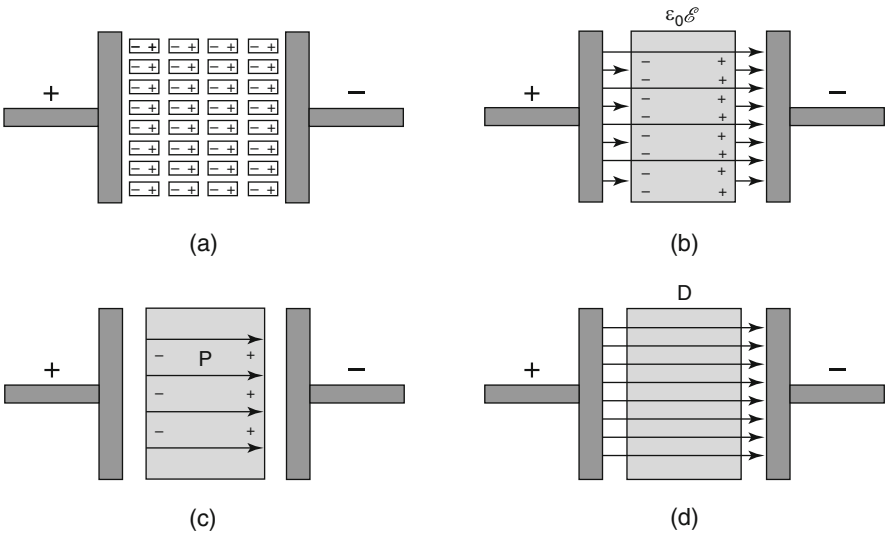

Figure 9.18. Schematic representation of two capacitor plates between which a dielectric material is inserted. (a) Induction of electric dipoles of opposite charge. (b) Weakening of the electric field *within* the dielectric material [Eq. (9.13)]. (c) The direction of the polarization vector is from the negative induced charge to the positive induced charge see Fig. 9.17(b). (d) The dielectric displacement, D, within the dielectric material is the sum of $\varepsilon_0\mathscr{E}$ and P [Eq. (9.15)].

where P is called the **dielectric polarization**, that is, the induced electric dipole moment per unit volume [Fig. 9.18 (c and d)]. The units for D and P are C m^{-2}; see Eq. (9.14). (D, $\mathscr{E}$, and P are generally vectors.) In summary, the polarization is responsible for the increase in charge density (q/A) above that for vacuum.

The mechanism just described is known by the name **electronic polarization**. It occurs in all dielectric materials that are subjected to an electric field. In ionic materials, such as the alkali halides, an additional process may occur, which is called **ionic polarization**. In short, cations and anions are somewhat displaced from their equilibrium positions under the influence of an external field and thus give rise to a net dipole moment. Finally, many materials already possess permanent dipoles that can be *aligned* in an external electric field. Among them are water, oils, organic liquids, waxes, amorphous polymers, polyvinylchloride, and certain ceramics, such as barium titanate ($BaTiO_3$). This mechanism is termed *orientation polarization*, or **molecular polarization**. All three polarization processes are additive if applicable; see below and Fig. 9.19.

Most capacitors are used in alternating electric circuits. This requires the dipoles to reorient quickly under a rapidly changing electric field. Not all polarization mechanisms respond equally quick to an alternating electric field. For example, many molecules are relatively sluggish in reorientation.

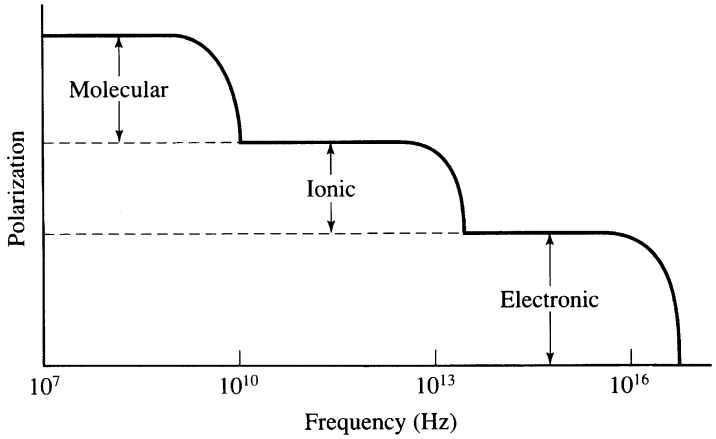

Figure 9.19. Schematic representation of the polarization as a function of excitation frequency for different polarization mechanisms. (A further mechanism, called "space charge polarization" which occurs at interphases between impurities and the matrix, and at grain boundaries withstands frequencies up to only 0.1 to 1 Hz. This is not shown here because of its relative unimportance for capacitors).

Thus, molecular polarization breaks down already at relatively low frequencies; see Fig. 9.19. In contrast, electronic polarization responds quite rapidly to an alternating electric field even at frequencies up to about 10^{16} Hz.

At certain frequencies a substantial amount of the excitation energy is absorbed and transferred into heat. This process is called *dielectric loss*. It is imperative to know the frequency for dielectric losses for a given material so that the respective device is not operated in this range.

9.6. Ferroelectricity, Piezoelectricity, Electrostriction, and Pyroelectricity

Certain materials, such as barium titanate, exhibit spontaneous polarization without the presence of an external electric field. Because these materials have electrical dipoles, their dielectric constants may be orders of magnitude larger than those of non-polar dielectrics (see Table 9.1). Thus, they are quite suitable for the manufacturing of small-sized, highly efficient capacitors. A **ferroelectric** material is a material in which these dipoles can be reoriented using an external electrical field. Specifically, if a ferroelectric material is exposed to a strong electric field, $\mathscr{E}$, its permanent dipoles become increasingly aligned with the external field direction until

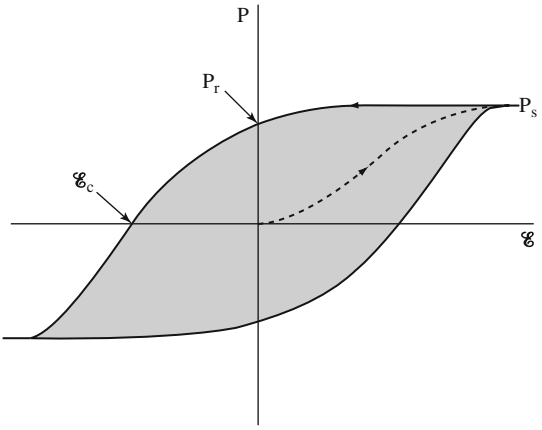

Figure 9.20. Schematic representation of a hysteresis loop for a *ferroelectric* material in an electric field. Compare to Fig. 15.6.

eventually all dipoles are as close to parallel to the field as possible and saturation of the polarization, P_s, is achieved, as depicted in Fig. 9.20. Once the external field has been withdrawn, a **remanent polarization**, P_r, remains which can only be removed by inverting the electric field until a coercive field, $\mathscr{E}_c$, is reached (Fig. 9.20). By further increasing the reverse electric field, orientation of the dipoles in the opposite direction is achieved. Finally, when reversing the field once more, a complete **hysteresis loop** is obtained, as depicted in Fig. 9.20. Therefore, ferroelectrics can be utilized for memory devices in computers, etc. The area within a hysteresis loop is proportional to the energy per unit volume that is dissipated once a full field cycle has been completed.

It should be emphasized at this point that ferroelectrics do not necessarily contain iron, as the name might suggest. Instead, the name is derived from the similarity of some properties of ferroelectric substances to those of ferromagnetic materials such as iron. In other words, ferroelectricity is the electric analogue to ferromagnetism, which will be discussed in Section 15.1.3.

A critical temperature, called the **Curie temperature**, exists, above which the ferroelectric effects are destroyed and the material becomes paraelectric. Typical Curie temperatures range from $-200°C$ for strontium titanate to at least $640°C$ for $NaNbO_3$.

The question that remains to be answered is, how do certain materials such as $BaTiO_3$ possess spontaneous polarization? This can be explained by recognizing that in the tetragonal crystal structure of $BaTiO_3$, the negatively charged oxygen ions and the positively charged Ti^{4+} ion are slightly displaced from their symmetrical positions, as depicted in Fig. 9.21. This results in a permanent ionic dipole moment along the *c*-axis within the

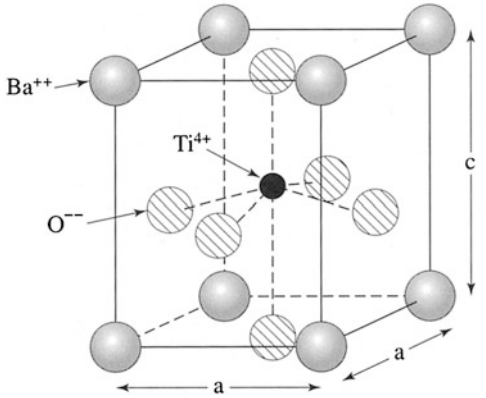

Figure 9.21. Tetragonal crystal structure of barium titanate at room temperature. Note the upward displacement of the Ti^{4+} ion in the center compared to the downward displacement of all surrounding O^{2-} ions. $a = 0.398$ nm; $c = 0.403$ nm.

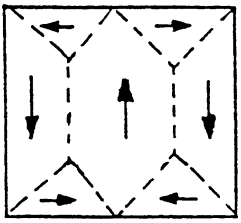

Figure 9.22. Schematic representation of spontaneous alignments of electric dipoles within a domain and random alignment of the dipole moments of several domains in a ferroelectric material such as $BaTiO_3$. Compare to Fig. 15.9.

unit cell. A large number of such dipoles line up in clusters (also called *domains*); see Fig. 9.22. In the virgin state, the polarization directions of the individual domains are, on average, randomly oriented, so that the material has no net polarization. An external field eventually orients the dipoles of the favorably oriented domains parallel to $\mathscr{E}$. Specifically, those domains in which the dipoles are already nearly parallel to $\mathscr{E}$ grow at the expense of unfavorably oriented domains.

By heating $BaTiO_3$ above its Curie temperature (120°C), the tetragonal unit cell transforms into a cubic cell whereby the ions now assume symmetric positions. Thus, no spontaneous alignment of dipoles remains, and $BaTiO_3$ is no longer ferroelectric.

If pressure is applied to a ferroelectric material, such as $BaTiO_3$, a change in the magnitude of the just-mentioned polarization may occur, which results in a small voltage across the sample. This effect is called

piezoelectricity.[20] It is found in a number of materials, such as quartz (though much weaker than in $BaTiO_3$), ZnO, and complex ceramic compounds such as $Pb(Zr,Ti)O_3$ (called PZT) and lead-free $Bi_{0.5}Na_{0.5}TiO_3$ and $K_{0.5}Na_{0.5}NbO_3$. Piezoelectricity is utilized in devices that are designed to convert mechanical strain into electricity. Those devices are called **transducers**. Applications include strain gages, microphones, sonar detectors, and phonograph pickups, to mention a few.

The piezoelectric effect in which stress is used to generate voltage is referred to as the **direct piezoelectric effect**. The converse mechanism, in which an applied electric field produces a change in dimensions in a ferroelectric material, is called the **converse piezoelectric effect**. The magnitude of such an effect may be up to 6×10^{-10} m/V for some of the $Pb(Zr,Ti)O_3$ materials. Examples of devices utilizing this effect include earphones, ink jet printer heads, and diesel fuel injectors. Probably the most important application, however, is the quartz crystal resonator, which is used in electronic devices as a *frequency selective element*. Specifically, a periodic strain is applied to a quartz crystal by an alternating electric field, which excites this crystal to vibrations. These vibrations are monitored, in turn, by piezoelectricity. If the applied frequency coincides with the natural resonance frequency of the molecules, then amplification occurs. This way, very distinct frequencies are produced, which are utilized for clocks or radio frequency signals.

Another phenomenon through which an electric field generates a change in dimensions is **electrostriction**. Electrostriction is a quadratic effect between electric field and mechanical strain, whereas piezoelectricity obeys a linear relationship. Electrostriction can be observed in all dielectric materials.

A related effect is **pyroelectricity**[21] which is observed in certain materials such as GaN, $CsNO_3$, polyvinyl fluorides, $LiTaO_3$, tendons, bones, and tourmaline (a silicate containing Al, Fe, Mg, Na, Li, or K). It describes a temporary voltage across the ends of these materials when the *entire* substance is heated or cooled. The change in temperature causes a variation of the polarization. The voltage, however, disappears after some time, due to current leakage. Pyroelectric materials are also piezoelectric. The reverse is not always true. Pyroelectricity was first described by Theophrastus in 314 BC who observed that tourmaline attracted small pieces of ash and straw when heated. In closing it is emphasized that pyroelectricity is not the same as thermoelectricity which we discussed in Section 7.7 where only one end is heated.

[20] Piezo (latin) = pressure.

[21] Pyr (greek) = fire.

Problems

1. Calculate the mobility of the oxygen ions in UO_2 at 700 K. The diffusion coefficient of O^{2-} at this temperature is 10^{-13} cm^2/s. Compare this mobility with electron or hole mobilities in semiconductors (see Appendix 4). Discuss the difference! (*Hint*: O^{2-} has two charges!).
2. Calculate the number of vacancy sites in an ionic conductor in which the metal ions are the predominant charge carriers. Assume a room-temperature ionic conductivity of 10^{-17} $1/\Omega$ cm and an ionic mobility of 10^{-17} m^2/V s. Does the calculated result make sense? Discuss how the vacancies might have been introduced into the crystal.
3. Calculate the activation energy for ionic conduction for a metal ion in an ionic crystal at 300 K. Take $D_0 = 10^{-3}$ m^2/s and $D = 10^{-17}$ m^2/s.
4. Calculate the ionic conductivity at 300 K for an ionic crystal. Assume 6×10^{20} Schottky defects per cubic meter, an activation energy of 0.8 eV and $D_0 = 10^{-3}$ m^2/s.
5. Show that $\mathscr{E} = \mathscr{E}_{vac}/\varepsilon$ [Eq. (9.13)] by combining Eqs. (7.3), (9.9), and (9.11) and their equivalents for vacuum.
6. Show that the dielectric polarization is $P = (\varepsilon - 1)\varepsilon_0\mathscr{E}$. What values do P and D have for vacuum?
7. Show that $\varepsilon\varepsilon_0\mathscr{E} = q/A$ [Eq. (9.14)] by combining some pertinent equations.

Suggestions for Further Reading (Part II)

N.W. Ashcroft and N.D. Mermin, *Solid State Physics*, Hold, Rinehart and Winston, New York (1976).
A.R. Blythe, *Electrical Properties of Polymers*, Cambridge University Press, Cambridge (1979).
M.H. Bordsky, ed., *Amorphous Semiconductors*, Springer-Verlag, Berlin, (1979).
I. Brodie and J. Muray, *The Physics of Microfabrication*, Plenum Press, New York (1982).
R.H. Bube, *Electronic Properties of Crystalline Solids*, Academic Press, New York (1974).
R.H. Bube, *Electrons in Solids*, 3rd ed., Academic Press, New York (1992).
J. Czochralski, Z. Physik. Chem. *92*, 219 (1918).
W.C. Dash, J. Appl. Phys. *30*, 459 (1959).
J.R. Ferraro, and J.M. Williams, *Introduction to Synthetic Electrical Conductors*, Academic Press, Orlando (1987).
S.K. Ghandi, *The Theory and Practice of Microelectronics*, Wiley, New York (1968).
S.K. Ghandi, *VLSI Fabrication Principles*, Wiley, New York (1983).
N.J. Grant and B.C. Giessen, eds., *Rapidly Quenched Metals*, Second International Conference. The Massachusetts Institute of Technology, Boston, MA (1976).
C.R.M. Grovenor, *Materials for Semiconductor Devices*, The Institute of Metals (1987).
L.L. Hench and J.K. West, *Principles of Electronic Ceramics*, Wiley, New York (1990).
B.H. Kear, B.C. Giessen, and K.M. Cohen, eds., *Rapidly Solidified Amorphous and Crystalline Alloys*, North-Holland, Amsterdam (1982).
C. Kittel, *Introduction to Solid State Physics*, 8th ed., Wiley, New York (2004).
J. Mort and G. Pfister, eds., *Electronic Properties of Polymers*, Wiley, New York (1982).

G.W. Neudeck and R.F. Pierret, eds., *Modular Series on Solid State Devices*, Vols. I–VI, Addison-Wesley, Reading, MA (1987).
M.A. Omar, *Elementary Solid State Physics*, Addison-Wesley, Reading, MA (1978).
A. Rocket, *The Materials Science of Semiconductors,* Springer-Verlag, New York, (2008)
D.A. Seanov ed., *Electrical Properties of Polymers*, Academic Press, New York, (1982).
B.G. Streetman and Sanjay Banerjee, *Solid State Electronic Devices*, 6th ed., Prentice-Hall, Englewood Cliffs, NJ (2006).
S.M. Sze and K.K. Ng, *Physics of Semiconductor Devices*, 3rd ed., Wiley, New York (2007).
S.M. Sze, *Semiconductor Devices, Physics and Technology*, Wiley, New York (1985).
H.E. Talley and D.G. Daugherty, *Physical Principles of Semiconductor Devices*, Iowa University Press, Ames, IA (1976).
L.H. Van Vlack, *Physical Ceramics for Engineers*, Addison-Wesley, Reading, MA (1964).
C.A. Wert and R.M. Thompson, *Physics of Solids*, 2nd ed., McGraw-Hill, New York (1970).
P.Y. Yu, and M. Cardona, *Fundamentals of Semiconductors-Physics and Materials Science,* 4th ed. Springer-Verlag, Berlin Heidelberg, (2010).